

# **AUTOMATING SINGLE SUBUNIT COUNTING OF MEMBRANE PROTEINS IN MAMMALIAN CELLS\***

**Hugo McGuire<sup>‡,§,1</sup>, Mark R. P. Aourousseau<sup>‡,1</sup>, Derek Bowie<sup>‡,1</sup> and Rikard Blunck<sup>‡,§,¶</sup>**

<sup>‡</sup>Groupe d'Étude des Protéines Membranaires (GÉPROM), Departments of <sup>§</sup>Physics and <sup>¶</sup>Physiology,  
Université de Montréal, Montréal, QC, H3C 3J7 and

<sup>1</sup>Department of Pharmacology and Therapeutics, McGill University, Montréal, QC, H3G 0B1, Canada

<sup>1</sup> *Both authors contributed equally to this work*

\*Running Title: *Automated Subunit Counting of Membrane Proteins*

To whom correspondence should be addressed: Dr. Rikard Blunck, Département de physique, C.P. 6128  
succ. Centre-ville, Université de Montréal, Montréal, QC, H3C 3J7, Email: rikard.blunck@umontreal.ca

**Key words:** single-molecule; step detection; ionotropic glutamate receptors; cys-loop receptors;  
superfolder GFP

## **SUPPLEMENTAL INFORMATION**

## SUPPLEMENTAL TEXT

### STEP DETECTION DETAILS OF PIF

#### Estimating noise

The basis of step detection by PIF rests on the ability to estimate the noise of a given trace in order to separate it from the bleaching steps. In brief, the noise is used as a “baseline” which a true step has to overcome in order to be recognized. In theory, the noise of a trace can be determined by calculating the difference between the parental raw trace and its idealization (noise free trace). The standard deviation of this resulting subtracted trace would reveal the global noise. However, it is impossible to obtain the idealized trace *a priori* because the idealized trace follows a baseline decreasing in discrete steps. Therefore, we estimated the noise using the standard deviation of the fluorescence fluctuations, as follows:

$$N_{FF} = \left( \frac{1}{T-1} \sum_{i=1}^{T-1} [\delta I - \bar{I}_{FF}]^2 \right)^{1/2} \quad \text{with} \quad \bar{I}_{FF} = \frac{I_T - I_1}{T-1} \quad (\text{eq. S1})$$

$$N_{FF} = \sqrt{\langle \delta I^2 \rangle - \langle \delta I \rangle^2} \quad (\text{eq. S1b})$$

where  $I_i$  is the fluorescence intensity of the frame  $i$ ,  $\bar{I}_{FF}$  represents the mean value of fluorescence fluctuations  $\delta I = (I_{i+1} - I_i)$ ,  $N_{FF}$  is the noise from “fluorescence fluctuations” and  $T$  is the total number of frames within a recording. Since these fluctuations should represent the direct random nature of noise measured directly,  $\bar{I}_{FF}$  is  $\sim 0$ . However, photobleaching events contribute to  $\bar{I}_{FF}$  to a negative value. If  $k$  steps of height  $\Delta I$  occur,  $I_{FF} \approx -k \Delta I / (T-1)$ . This would be exactly the expected value for each fluctuation, were the decay continuously distributed over each sample point.

Although this calculation tends to overestimate the noise of a trace, the precise knowledge of the noise is not essential since step detection was optimized with reference to the definition of  $N_{FF}$  here. More precisely, the optimal step detection sensitivity  $\phi$ , which represents the basis of the step detection algorithm (*see below*), was determined using simulated trace data where  $N_{FF}$  is controlled.  $\phi$  is expressed as a function of the signal-to-noise ratio  $SNR$ , using the step amplitudes as the signal and  $N_{FF}$  as noise

#### Progressive Step Detection

Although  $N_{FF}$  is initially known, we would also need the yet-unknown step amplitudes to evaluate the  $SNR$  of the trace. To circumvent this obstacle, the algorithm starts with a very small value for the  $SNR$  (user-defined parameter to  $\sim 0.25$ -1.0) and thus for the  $signal = SNR \cdot N_{FF}$ . The step detection algorithm compares the current fluctuations to a threshold factor  $\sigma = signal / \phi$ , where  $\phi$  is defined as the step detection sensitivity  $\phi$ .  $\phi$  is an empirical calibration factor relating the step threshold  $\sigma$  to the current signal to noise ratio  $SNR$ . The step detection sensitivity  $\phi$  is well described by an exponential function that starts saturating for  $SNR > \sim 2.5$  (Supplemental Fig. 1C). To keep the initial threshold  $\sigma$  small,  $SNR$  is set to a small and by association  $\phi$  to a large value. Initially, the threshold is set to an even much smaller value  $\sigma_1 = \sigma/1000$  (*see Annealing phase below*).

The step detection algorithm itself progresses in an iterative manner and can be broken down into the three major steps described below (Supplemental Fig. 2).

1. **SCANNING PHASE:** The first data point is set as reference. Starting from here, the algorithm compares the intensity of each subsequent point to that of the reference. Three outcomes are possible; (i) If a point of larger intensity than the reference is found, all data points between the reference and this larger one are set to their average intensity; these points create one idealized “level” (Supplemental Fig. 2A). Then the algorithm proceeds to the next data point, which is set as new reference and begins a new level. Subsequent points are compared to this new reference. (ii) If the value of any subsequent point is lower than the reference but their difference still smaller than the threshold ( $I_{reference} - I_i < \sigma_I$ ), the algorithm sets all points between the reference to the current one to their average intensity (Supplemental Fig. 2B). The reference obtains a new value, but the *same* level is continued with the next data point. (iii) Finally, if the intensity falls below the reference by more than the threshold, the previous level is ended. This lower point itself becomes the new reference and the following points are compared to it (Supplemental Fig. 2C). The algorithm continues to the end of the trace and is then restarted with the idealized (“leveled”) data points with identical  $\sigma$ . This is repeated until the number of levels is no longer decreased (Supplemental Fig. 2, D and E).
2. **ANNEALING PHASE:** Once the idealization for a given threshold value no longer changes, the threshold is progressively increased ( $\sigma_{I...}\sigma_{1000} = \sigma/1000, \sigma/999, \sigma/998, \dots$ , to  $\sigma$ ) and each time the scanning phase repeated on the previous idealization (Supplemental Fig. 2F). Although one might think that the result should be similar to directly using the final value of  $\sigma$  defined through  $SNR$  and  $\phi$ , it turned out that the accuracy was higher if the system was allowed to slowly anneal its final sensitivity.
3. **REEVALUATION:** Once the levels are no longer reduced even with the final value of  $\sigma$ , the new idealized values are used to re-compute  $N_{FF}$ . Now, also “signals”, step heights between levels, are available, so that  $SNR$  and  $\phi$  can be re-evaluated. With these values and the current idealized data points, scanning and annealing phase are repeated on the previous idealization – again until levels are no longer reduced (Supplemental Fig. 2G).

Initially, many small fluctuations are interpreted as steps (Supplemental Fig. 2D, *left*). By association all three step amplitudes,  $SNR$  and  $\sigma$  remain small, too. With progressing idealization, the number of levels decreases and step amplitudes increase until finally only the “real” photobleaching steps overcome the threshold  $\sigma$ . The algorithm, however, does not actually aim to detect steps, but inversely scans for periods of constant intensity.

The slow progression reduces the probability of detecting variations in the trace due to noise or blinking events as photobleaching events. Also, the slow progression reduces the probability of missing low amplitude photobleaching events. Despite the algorithm’s iterative nature, final idealizations are generally obtained within fractions of a second using a modern PC. The computing time decreases with increasing idealization as only differences between levels are evaluated and not each data point.

## TRACE REJECTION

The step detection algorithm will attempt to find step-wise behaviour in any provided trace, even though that trace may not actually contain any steps. Therefore, after step detection, traces must be evaluated by a set of criteria as an estimate of trace quality. Five criteria were implemented into PIF for the evaluation of the step-wise behaviour: Thresholds for the maximal Chi-squared, for *SNR*, for the maximal time allowed for all fluorophores to bleach and for the maximal step amplitude.

- a. The Chi-squared ratio between the actual fit and a counter-fit for a given trace is a strong indicator of the step-wise behaviour. The counter-fit is computed as the average value between the centers of adjacent levels, as if the steps were located in the middle of two real consecutive steps (1). Small Chi-squared values are indicative of a better fit, and high values, such as those expected of a counter-fit, are indicative of poor fits. Consequently, a high ratio ( $> 1$ ) between chi-squared values of the counter-fit and of the actual fit generally correspond to traces exhibiting clear step-wise behaviour (1). Accordingly, a ratio  $< 1$  implies that the counter-fit is a better representation of the trace than the actual fit itself. Therefore, traces with a ratio  $< 1$  are excluded from analysis.
- b. Evaluating the quality of the fit for a given trace is achieved by calculating a Chi-squared value for the fit. The ability of PIF to fit a trace that does not exhibit clear step-wise behaviour (e.g. resulting from random fluorescence variations) is poor. In such cases, a goodness of fit ( $\chi^2_{fit}$ ) based on a Chi-squared calculation can be evaluated as follows:

$$\chi^2_{fit} = \sum_i \frac{(Exp_i - Ideal_i)^2}{var_i} \quad (eq. S3)$$

where  $Exp_i$  and  $Ideal_i$  represent the data and the idealization at frame  $i$ , respectively. After idealization, the variance  $var$  is calculated for each intensity level found. If the trace contains too many false detections or missed events,  $\chi^2_{fit}$  is expected to be smaller or larger than 1, respectively. False detections are generally not observed in our measurements because only the step-wise behaviour is fitted, not the blinking events or any imperfection within the trace. As a result, the threshold for rejection by the goodness of fit  $\chi^2_{fit}$  was empirically determined to be 1.5

- c. Simulation experiments established that the accuracy of step detection of PIF is significantly reduced in traces where the SNR is  $< \sim 2.5$  after applying C-K filtering (corresponding to  $\sim 0.85$  in the raw trace). Therefore, SNR was used as a rejection criterion where traces with SNRs  $< 2.5$  after filtering were discarded. This should not influence the resulting step distributions because the SNR is independent of the step number. In experimental data almost every trace had SNRs above 2.5 after applying the C-K filter (Supplemental Fig. 1B).
- d. The fourth criterion is based on the time required to bleach  $n$  fluorophores, which is set using the lifetime of the fluorophores. To determine this lifetime, an exponential decay curve is fitted to the summed intensity of all selected spots within a region of interest. This decay leads directly to the probability fulfilled by any fluorophore that it has photobleached after excitation time  $t$ :

$$P_{bleach}(t) = (1 - e^{-t/\tau}) \quad (eq. S4)$$

From this relation, one can compute the time required to have a probability  $P_{time}(n)$  of getting all  $n$  fluorophores photobleached:

$$P_{time}(n) = \left(1 - e^{t/\tau}\right)^n \quad (eq. S5)$$

$$t = -\tau \cdot \ln\left(1 - P_{time}^{1/n}\right) \quad (eq. S6)$$

The last relation can be used to determine the time when with a certain probability  $P_{time}$  all fluorophores have photobleached dependent on the number of steps detected. If a trace still shows steps after this allowed period of time, it is rejected. We found that setting  $P_{time}$  between 90% and 95% does not appear to reject clear traces, but mainly those where the exponential decay background was not successfully removed, leading to detection of *false* steps typically towards the end of the traces. It also helps to reject contaminant spots, as they are often represented as “unclear” single photobleaching step traces with long duration.

- e. This single photobleaching event of the background fluorescence often exhibited an amplitude that was consistently significantly larger than steps attributed to the photobleaching of the fluorophores. These contaminants were removed by setting a rejection criterion based on the maximum allowable step amplitude. Traces showing step amplitudes greater than 2550 arb.u. (~3 times the amplitude of the average step size obtained from a step amplitude distribution) were rejected (Supplemental Fig. 3E).

### ***CALCULATING THE PROBABILITY OF MISSED EVENTS***

As missed photobleaching events could have an influence on the step frequency distribution (see Supplemental Fig. 3B), here we show the derivation of the probability of missing a photobleaching event ( $P_{miss}(\Delta t)$ ) for a given time resolution  $\Delta t$ . As during  $\Delta t$  only a single step may be detected even though 2 or more occurred,  $P_{miss}$  is described by the probability that 2 or more photobleaching events occurred within the same interval  $\Delta t$ , while the other remaining fluorophores do not photobleach during this time interval. To evaluate this, the previously described probability  $P_{bleach}(t)$  is used as a starting point. This probability represents the cumulative probability distribution of the probability density function  $P_d(t)$  as follow:

$$P_d(t) = \frac{d}{dt} P_{bleach}(t) = \frac{e^{-t/\tau}}{\tau} \quad (eq. S7)$$

$P_d(t)$  is useful to determine the probability that a fluorophore photobleaches during a given time interval by a simple integration. For instance, the integral of  $P_d(t)$  between 0 and  $t$  returns the relation  $P_{bleach}(t)$ , as it represents the probability of being photobleached after time  $t$ . Also, the integral from 0 to infinity results to 1, as the fluorophore will photobleach eventually. From this probability density, we estimate the probability of missing 1 photobleaching event by the multiplication of the probability that 2 fluorophores photobleach during the same time interval  $i$  [ $t_i, t_i + \Delta t$ ] and the probability that the other  $n-2$  remaining fluorophores do not photobleach during this time interval, as shown in the equation S8. Finally, all time intervals  $i$  must be summed up to consider the whole trace. As fluorophores are not distinguishable, we have to consider their permutation as another multiplicative factor

$$\begin{aligned}
P_{miss}^1(\tau, \Delta t) &= \sum_i \frac{n!}{2!(n-2)!} \left( \int_{t_i}^{t_i+\Delta t} \frac{e^{-t/\tau}}{\tau} dt \right)^2 \left( 1 - \int_{t_i}^{t_i+\Delta t} \frac{e^{-t/\tau}}{\tau} dt \right)^{n-2} \\
&= \sum_i \frac{n!}{2!(n-2)!} \left( e^{-t_i/\tau} (1 - e^{-\Delta t/\tau}) \right)^2 \left( 1 - e^{-t_i/\tau} (1 - e^{-\Delta t/\tau}) \right)^{n-2}
\end{aligned} \tag{eq. S8}$$

To calculate the probability of missing  $k-1$  events, the formula has to be adjusted in the following way:

$$P_{miss}^{k-1}(\tau, \Delta t) = \sum_i \frac{n!}{k!(n-k)!} \left( e^{-t_i/\tau} (1 - e^{-\Delta t/\tau}) \right)^k \left( 1 - e^{-t_i/\tau} (1 - e^{-\Delta t/\tau}) \right)^{n-k} \tag{eq. S9}$$

So, the probability of missing 1 or more photobleaching events is the sum of all the possibilities:

$$P_{miss}(\tau, \Delta t) = \sum_{k=2}^n \left( \sum_i \frac{n!}{k!(n-k)!} \left( e^{-t_i/\tau} (1 - e^{-\Delta t/\tau}) \right)^k \left( 1 - e^{-t_i/\tau} (1 - e^{-\Delta t/\tau}) \right)^{n-k} \right) \tag{eq. S10}$$

In typical experiments, the lifetime  $\tau$  is approximately 7 s and  $\Delta t = 150$  ms. For  $n = 5$  existing fluorophores, we then estimate  $P_{miss}$  to about 10.4%. If  $n = 4$  or  $n = 3$ ,  $P_{miss}$  is calculated to be about 6.3% and 3.2%, respectively.

Simulations using  $\tau = 7$  s and  $\Delta t = 150$  ms were also done to estimate  $P_{miss}$ . 500 photobleaching traces were simulated 5 times for  $n = 5$ ,  $n = 4$  and  $n = 3$ . Each fluorophore was associated to a 2-state Markov model where the transition from the fluorescent state and the photobleached state occurs according to the rate constant  $1/\tau$ . Missed events were observed when 2 or more fluorophores photobleached within the same time resolution  $\Delta t$ . The results correspond nicely to the previous calculation. For  $n = 5$ ,  $n = 4$  and  $n = 3$ ,  $P_{miss}$  was obtained to be  $10.1 \pm 1.3\%$ ,  $6.4 \pm 0.8\%$  and  $2.8 \pm 1.1\%$ , respectively.

## REFERENCES

1. Kerssemakers, J. W., Munteanu, E. L., Laan, L., Noetzel, T. L., Janson, M. E., and Dogterom, M. (2006) Assembly dynamics of microtubules at molecular resolution. *Nature* **442**, 709-712

## FIGURE LEGENDS

**Supplemental Figure 1.** (A) Illustration of the Markov model used to simulate photobleaching data. Only single transition blinking is allowed, described by the rate constants  $\alpha$  and  $\beta$ . These two parameters respectively define the transition of a fluorophore from a non-fluorescent to a fluorescent state, and vice versa. The last parameter, the rate constant  $\kappa$ , describes the transition of a fluorophore from a fluorescent state to its photobleaching and is therefore unidirectional. The model allows up to 11 fluorophores, but it is possible to start from a state where  $x$  ( $<11$ ) fluorophores are left (not photobleached) in order to simulate traces with different step number. (B) Effect of C-K filtering on the signal-to-noise ratio. Chung-Kennedy filter has the ability to increase the signal-to-noise ratio of a trace while keeping a steep edge for relevant intensity variations. To evaluate the effect of C-K filtering on SNR, we used the fully-automated analysis of msfGFP-GluK2, as the SNR was computed with and without C-K filtering for the same idealization. The resulting distributions reveal a SNR increase by a factor of approximately  $3.0 \pm 0.5$ . (C) The sensitivity  $\phi$  used in the step detection algorithm was optimized from simulations by choosing the value corresponding to the larger accuracy for a given SNR.  $\phi$  was subsequently plotted as a function of SNR and fitted with a single exponential decay curve. The resulting exponential decay equation then became the calibration formula in the step detection algorithm. (D) Comparison of spots on-cell and off-cell and effect of LoG-type kernel filtering. Using a  $\delta F/F$  cut-off of 10%, the normalized intensity distributions on-cell (*blue*) and off-cell (*red*) are compared by calculating the average intensity of the spots over the first 100 frames (5 sec). From these distributions, the  $\delta F$  threshold was set to 1750 (arb.u.) for the actual system used. (E) The comparison in accuracy of PIF step detection and STEPFINDER is illustrated as a function of SNR. This evaluation was obtained using simulated traces containing 11 equidistant traces without blinking. Over the tested range of SNR, PIF reveals a larger accuracy than STEPFINDER. In the particular case of STEPFINDER, the accuracy was not precisely obtained for SNR lower than  $\sim 4$ , as the step distribution was very broad and accordingly very difficult to fit as previously described in “*Simulations: Calculation of the Accuracy  $p_{acc}$* ”. STEPFINDER detected step number was obtained by maximizing the ratio between the Chi-squared value of a counter-fit and the one corresponding to the fit (1).

**Supplemental Figure 2.** PIF step detection algorithm described as conditions for segment averaging (see text for details). These conditions are iteratively repeated over averaged segments until convergence of the idealization. The progression of the algorithm can be divided into three main sections (phase 1,2,3), which are illustrated for a simulated trace containing 11 steps. Each algorithm section gradually removes the false detections within the trace.

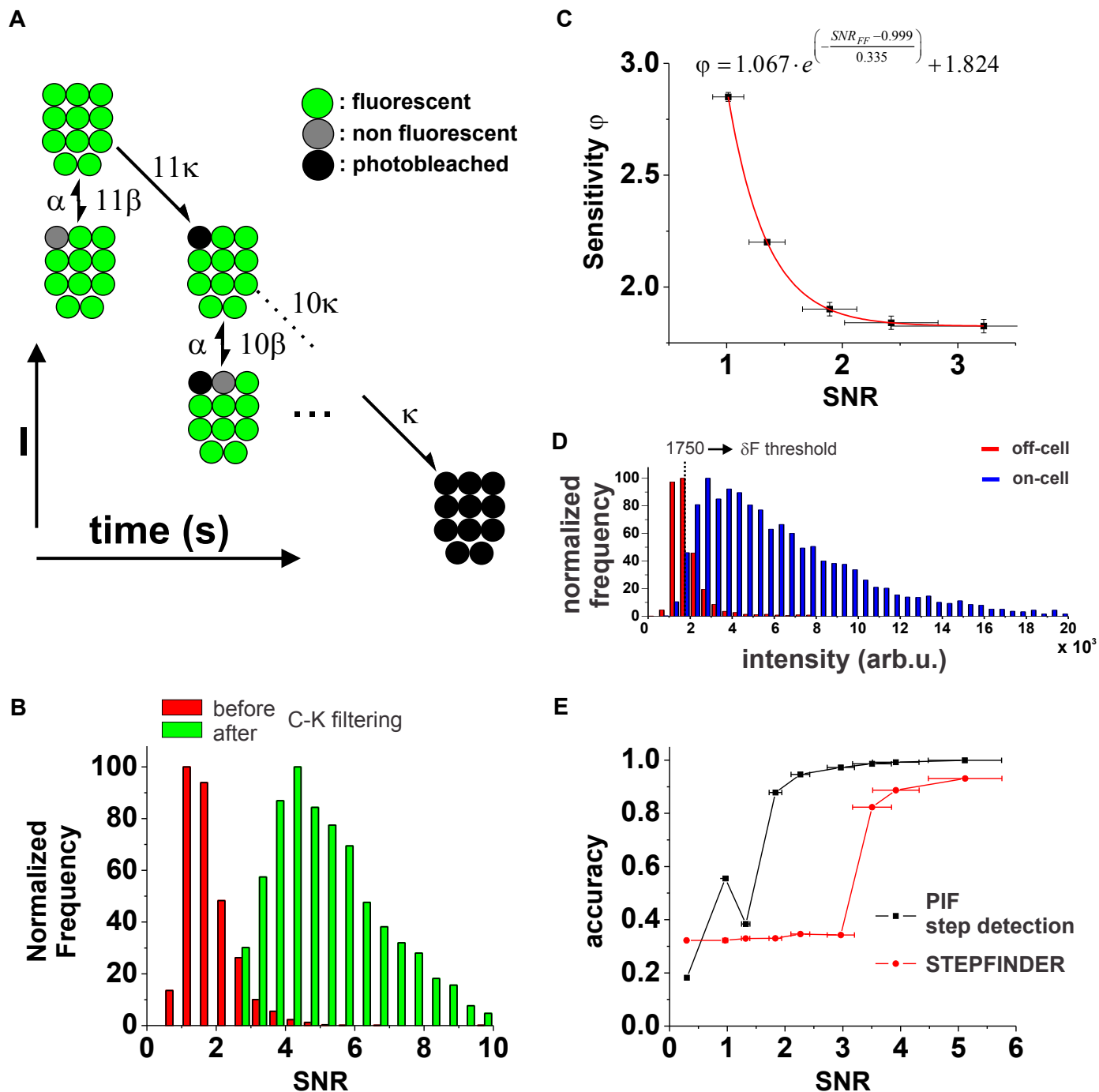
**Supplemental Figure 3.** (A-D) Effect of step detection parameters on PIF automated analysis over GluK2. Step detection parameters were optimized by adding each parameter one at a time to the previous settings, as to check their influence on the overall step distribution. (A) Step distribution without using the parameters, except for the minimum time between steps which has to be set to 2 frames by default (see *Step Detection*). (B) The minimum time between steps is set to 3 frames (150 ms). This tends to decrease the number of false detections possibly due to C-K filtering and slight changes in the baseline, likely produced by an incomplete background removal (see *Trace filtering* in main text). This restriction does not significantly alter the probability of missing a step event, which remains below  $\sim 6\%$  (see *Calculating the Probability of Missed Events* in the *Supplemental Text*). It is important to keep this value relatively small, as it could alter the final observed step distribution frequency by introducing a shift

toward smaller values. Depending on each situation, larger probabilities of missing a step might complicate the interpretation of the results. (C) the maximal step amplitude variation is in addition set to 60%. As false steps were small in comparison to the maximal step size detected within a trace, setting the maximal amplitude variation to 60% of the largest step effectively removed these artifacts. This limit still tolerates variations in amplitudes due to blinking events and allows the possibility of two fluorophores photobleaching during one frame exposure. (D) According to the step size distribution (see E), the minimum step size amplitude of 375 (arb.u.) is added to the previous settings, while traces containing steps over 2550 (arb.u.) are rejected. We found that the most common step amplitude detected in all the traces is about 750-850 (arbitrary units specific to our system, see E). Since excitation intensity remains uniform over the entire recorded field of view (maximum intensity variations of  $\sim 15\%$ ), we reasoned that it was unlikely to observe a fluorophore emitting less than half the intensity of the most commonly observed fluorescence intensity. Therefore, steps with intensities smaller than 375 (arb.u.) are attributed to artifacts of a decreasing baseline. Since concomitant multiple photobleaching steps are possible, though very infrequent, an upper step amplitude limit was also set as  $3 \times 850 = 2550$  (arb.u.). Traces containing steps outside this intensity range were rejected. (E) The step size distribution of detected steps was obtained from accepted traces of the distribution obtained in C.

**Supplemental Figure 4.** Effect of blinking on step detection accuracy. Sets of 500 simulated traces containing 4 photobleaching steps with different blinking properties were analyzed by PIF step detection algorithm for different SNRs. The accuracy curves using  $\alpha = 1$  (black squares), 5 (red triangles), 10 (green circles), 50 (blue stars) are illustrated for  $\beta = 0.1 \text{ s}^{-1}$  (*left*) and  $\beta = 1 \text{ s}^{-1}$  (*right*).

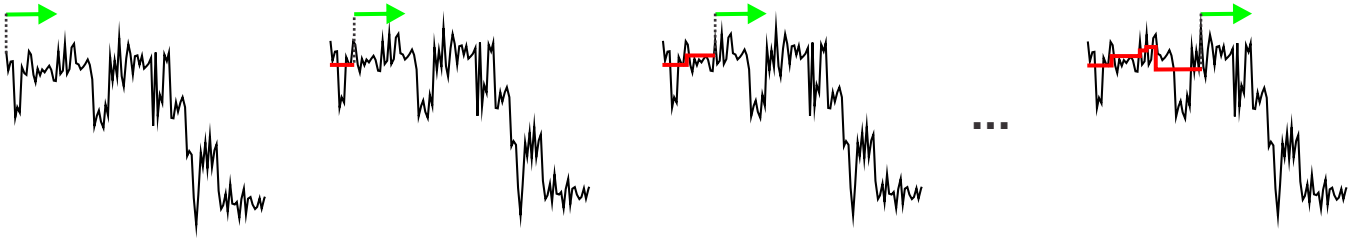


# Supplemental Figure 1

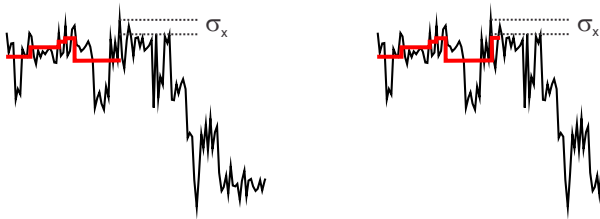


# Supplemental Figure 2

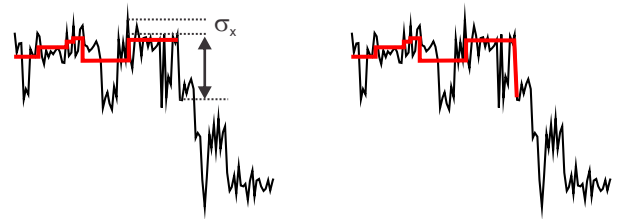
**A** if larger intensity is found  
then average segment



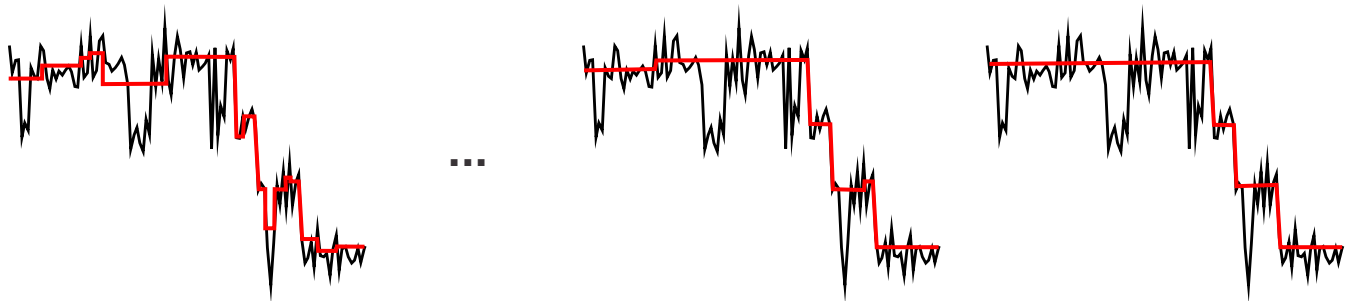
**B** if intensity drop  $< \sigma_x$   
then average segment



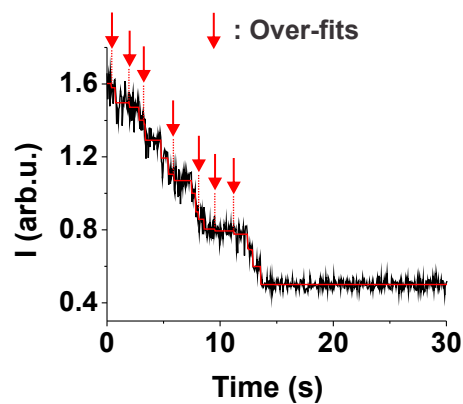
**C** last position where intensity drop  $< \sigma_x$   
level is ended; go to the next one



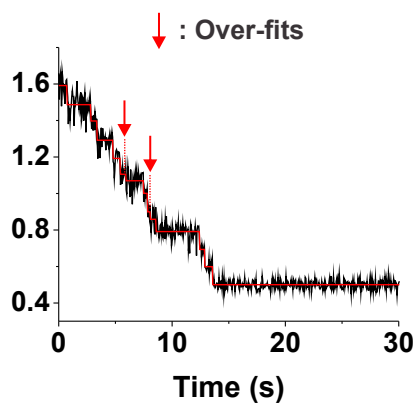
**D** After the whole trace is segmented, subsequent iterations start over using the  
previous averaged segments until the idealization no longer changes



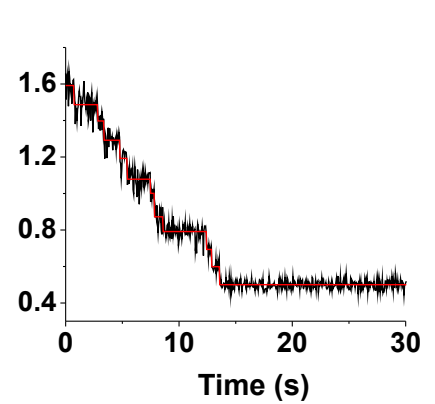
**E** phase 1



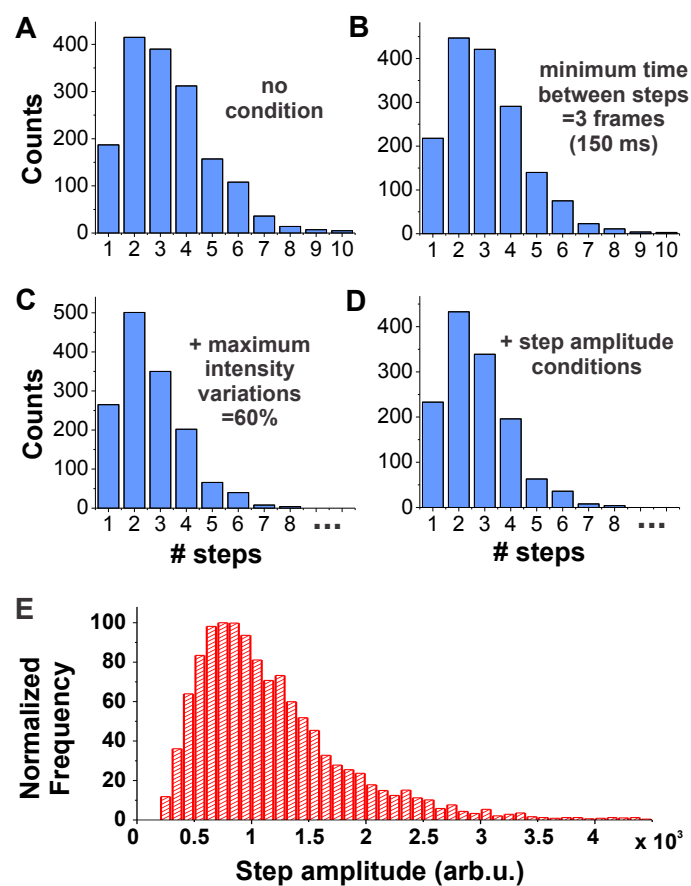
**F** phase 2



**G** phase 3



# Supplemental Figure 3



# Supplemental Figure 4

